Available online at www.sciencedirect.com
SCIENCE DIRECT®
Nuclear Instruments and Methods in Physics Research A 534 (2004) 531–543
NUCLEAR INSTRUMENTS & METHODS IN PHYSICS RESEARCH Section A
www.elsevier.com/locate/nima

Cold and thermal neutron scattering in liquid water: cross-section model and dynamics of water molecules

Yoshinobu Edura*, Nobuhiro Morishima

Department of Nuclear Engineering, Kyoto University, Yoshida-Honmachi, Sakyo-ku, Kyoto 606-8501, Japan

Received 18 May 2004; accepted 15 June 2004
Available online 9 August 2004

Abstract

A cross-section model for incoherent inelastic scattering of slow neutrons in liquid water is developed. The model is expressed basically in terms of a width function (a mean squared displacement of a water molecule) and, equivalently, a generalized frequency distribution (a vibrational density of states). The microscopic dynamics of water molecules is fully described from very general considerations connected with jump diffusion, intermolecular vibration, hindered rotation and intramolecular vibration. The model covers a wide time range of the order of 0.1 fs to 1 μs. Hence a full set of double-differential and total cross sections for neutron incident energies from 0.1 μeV to 10 eV is calculable. Satisfactory agreement with neutron-scattering and molecular-dynamics results is found at many different temperatures between 0 °C and 100 °C. This indicates the usefulness of the present model for generation of an advanced cross-section library for practical purposes.

PACS: 61.20.Lc; 61.25.Em; 78.70.Nx; 29.25.Dz

Keywords: Water; Neutron cross sections; Dynamics model; Dynamical relaxation; Cold neutron scattering; Neutron source

1. Introduction

Owing to the neutron scattering experiments [1–6] and the molecular dynamics simulations [7–11] in last two decades, dynamics of water molecules has been largely clarified, which may be summarized as follows:

- A water molecule is prevented from a simple self-diffusion by a hydrogen-bonds network formed with surrounding molecules [4].
- Translational diffusion and intermolecular vibration are repeated as a jump diffusion process [12]. The jump diffusion model for the

*Corresponding author. Tel./fax: +81-75-753-5836.
E-mail address: edura@nucleng.kyoto-u.ac.jp (Y. Edura).

0168-9002/$ - see front matter © 2004 Elsevier B.V. All rights reserved.
doi:10.1016/j.nima.2004.06.140

translation on a large time scale of, say, $\geqslant 1$ ps has been observed by the cold neutron scattering experiments performed by Teixeira et al. [1,2]. It has been also shown that there are two intermolecular vibrational modes, both bending and stretching, with characteristic energies of about 8 and 20 meV, respectively.

- Molecular rotational motion may be described in terms of the rotational diffusion based on the Sear's expansion [11,13,14] in a large time scale and the hindered rotation (librational vibration) with a broad distribution of energies centered about 80 meV in an intermediate time scale.
- Intramolecular vibration includes such three normal modes as bending, stretching and asymmetric-stretching. It depends on symmetries of the molecular shape of water. The characteristic energy of the bending mode is about 210 meV, and the ones of the stretching and asymmetric-stretching modes are in common about 460 meV [5,6].

Hence it is desirable to develop a cross-section model of neutron scattering in water molecules which includes all the above-mentioned dynamics systematically. Although several models have been presented so far, most of them are based on the free-gas description of molecular translation [15–17], the simple diffusion description [18,19] and the synthetic method for scattering functions [20–22]. In the present paper, a new cross-section model for slow neutron scattering in liquid water is proposed. It covers a wide range of neutron incident energies from 0.1 μeV (ultracold) to 10 eV (epi-thermal) and water temperatures from 0 °C to 100 °C. On the basis of a velocity autocorrelation function (VACF) $\langle v(0)v(t)\rangle$ and, equivalently, a generalized frequency distribution (GFD) (a vibrational density of states) $D(\omega)$, a variety of scattering functions are calculable: an intermediate scattering function (ISF) $I_s(Q,t)$, a self-scattering function (SSF) $S_s(Q,\omega)$, a double-differential scattering cross section (DDX) $d^2\sigma/d\Omega dE'$, an angular distribution (AD) $d\sigma/d\Omega$ and a total scattering cross section (TSX) $\sigma_s(E)$. This permits us to generate a set of well-defined cross-section libraries of water at many different temperatures. They will be necessary for practical purposes such as design and analysis of advanced neutron sources, and nuclear energy research and development. Another usefulness of the model lies in the possibility of serving for further study of physicochemical properties of liquid water being characterized by a hydrogen-bonded network.

Section 2 describes slow neutron scattering in water in terms of the various scattering functions mentioned above. On the basis of the recent physicochemical results by neutron scattering [1–6] and computer simulations [7–11], the cross-section model applicable to the wide range of neutron incident energies and liquid temperatures is developed. Section 3 demonstrates many different scattering properties by comparison with the neutron-scattering and computer-simulation results [2,3,8,23–29]. Section 4 is devoted to the concluding remarks. All the parameter values are listed in Table 1.

2. Cross-section model

2.1. Scattering functions

The DDX of a water molecule may be expressed using the SSF $S_s^X(Q,\omega)$ (X = H, O) by incoherent approximation:

$$\frac{d^2\sigma}{d\Omega dE'} = 2\frac{k'}{k}\frac{1}{\hbar}\left(\frac{\sigma_{coh}^H}{4\pi}+\frac{\sigma_{inc}^H}{4\pi}\right)S_s^H(Q,\omega) + \frac{k'}{k}\frac{1}{\hbar}\left(\frac{\sigma_{coh}^O}{4\pi}+\frac{\sigma_{inc}^O}{4\pi}\right)S_s^O(Q,\omega) \quad (1)$$

where $\hbar$ is the Planck's constant, k and k' are the wave numbers for incident and scattered neutrons, respectively, σ_{coh}^X and σ_{inc}^X are the bound-atom coherent and incoherent scattering cross sections, respectively, and Q and ω are the momentum and energy transfers defined as

$$\hbar\vec{Q} = \hbar\vec{k'} - \hbar\vec{k} \quad (2)$$

$$\hbar\omega = E' - E \quad (3)$$

with the energies E and E' for incident and scattered neutrons, respectively. Note that $\omega > 0$

Table 1
Physical constants and parameters for the present model

Definition	Symbol (Unit)	H	O
Atomic mass	M^{X} (meV ps^2 Å^{-2})	0.1044	1.658
Bound-atom coherent scattering cross section	$\sigma^{\mathrm{X}}_{\mathrm{coh}}$ (b atom^{-1})	1.759	4.232
Bound-atom incoherent scattering cross section	$\sigma^{\mathrm{X}}_{\mathrm{inc}}$ (b atom^{-1})	80.23	0.000
Absorption cross section	$\sigma^{\mathrm{X}}_{\mathrm{a}}$(b atom^{-1}) at 25 meV	0.3326	0.000
Translational diffusion (d)			
Diffusion coefficient	$D_{\mathrm{t}}(T)$ (Å^2 ps^{-1})	$258.2 \times \exp\left(-2.108\,\frac{1000}{T}\right)$	
Residence time	$\tau_0(T)$ (ps)	$1.548 \times 10^{-4} \times \exp\left(2.648\,\frac{1000}{T}\right)$	
Effective mass	$M^{\mathrm{X}}_{\mathrm{d}}(T)$ (meV ps^2 Å^{-2})	$\tau_0(T)k_{\mathrm{B}}T/D_{\mathrm{t}}(T)$	
Intermolecular vibration (t)			
Bending mode	$\varepsilon^{\mathrm{H}\,0}_{\mathrm{t}\,1}$ at 20 °C	0.016	
	$\varepsilon^{\mathrm{X}}_{\mathrm{t}\,1}(T)$, $\hbar\omega^{\mathrm{X}}_{\mathrm{t}\,1}$ (meV)	Eq. (55), 8.25	Eq. (57), 8.25
Stretching mode	$\varepsilon^{\mathrm{H}\,0}_{\mathrm{t}\,2}$ at 20 °C	0.028	
	$\varepsilon^{\mathrm{X}}_{\mathrm{t}\,2}(T)$, $\hbar\omega^{\mathrm{X}}_{\mathrm{t}\,2}$ (meV)	Eq. (55), 30.0	Eq. (57), 30.0
Rotational diffusion (RD)			
Rotational diffusion coefficient	$D_{\mathrm{r}}(T)$ (ps^{-1})	$(6\tau_{\mathrm{RD}}(T))^{-1}$	—
Rotational relaxation time	$\tau_{\mathrm{RD}}(T)$ (ps)	$0.0485 \times \exp\left(\frac{80.7}{k_{\mathrm{B}}T}\right)$	—
Bond length of H–O	R (Å)	0.91	—
Mass ratio	$M^{\mathrm{H}}/M^{\mathrm{H}}_{\mathrm{r}}$	0.0006	—
Hindered rotation (HR)	$\varepsilon^{\mathrm{H}\,0}_{\mathrm{HR}}$ at 20 °C	0.5548	
	$\varepsilon^{\mathrm{H}}_{\mathrm{HR}}(T)$, $\hbar\omega^{\mathrm{H}}_{\mathrm{HR}}$ (meV)	Eq. (56), 90.0	—
Intramolecular vibration (v)			
Bending mode	$\varepsilon^{\mathrm{X}}_{\mathrm{v}\,1}$, $\hbar\omega_{\mathrm{v}\,1}$ (meV), $\sigma_{\mathrm{v}\,1}$ (meV)	0.133, 210, 5.0	0.0233, 210, 5.0
Stretching mode	$\varepsilon^{\mathrm{X}}_{\mathrm{v}\,2}$, $\hbar\omega_{\mathrm{v}\,2}$ (meV), $\sigma_{\mathrm{v}\,2}$ (meV)	0.133, 460, 10.0	0.0233, 460, 10.0
Asymmetric-stretching mode	$\varepsilon^{\mathrm{X}}_{\mathrm{v}\,3}$, $\hbar\omega_{\mathrm{v}\,3}$ (meV), $\sigma_{\mathrm{v}\,3}$ (meV)	0.133, 460, 10.0	0.0233, 460, 10.0

where $\hbar = 0.6582\,\mathrm{meV\,ps}$ and $k_{\mathrm{B}} = 0.08617\,\mathrm{meV\,K^{-1}}$.

and $\omega < 0$ indicate energy-gain (up) and energy-loss (down) scattering, respectively.

The SSF is defined by the Fourier transform of the ISF $I^{\mathrm{X}}_{\mathrm{s}}(Q,t)$:

$$S^{\mathrm{X}}_{\mathrm{s}}(Q,\omega) = \frac{1}{2\pi}\int_{-\infty}^{\infty} I^{\mathrm{X}}_{\mathrm{s}}(Q,t)\exp(\mathrm{i}\omega t)\,\mathrm{d}t. \tag{4}$$

In the Gaussian approximation, the ISF can be written as

$$I^{\mathrm{X}}_{\mathrm{s}}(Q,t) = \exp\left[-\frac{1}{2}\,Q^2 W^{\mathrm{X}}(t)\right] \tag{5}$$

where $W^{\mathrm{X}}(t)$ is the width function (WF) and defined as the mean squared displacement $\langle \Delta r^2\rangle^{\mathrm{X}}$ of a water molecule during the period t:

$$W^{\mathrm{X}}(t) = \frac{1}{3}\,\langle \Delta r^2\rangle^{\mathrm{X}}. \tag{6}$$

Hence the VACF is obtained by

$$\langle v(0)v(t)\rangle^{\mathrm{X}} = \frac{3}{2}\lim_{Q\to 0}\frac{\mathrm{d}^2}{\mathrm{d}t^2}\,W^{\mathrm{X}}(t) \tag{7}$$

and the Fourier transform of the real part of the VACF gives the GFD $D^{\mathrm{X}}(\omega)$:

$$D^{\mathrm{X}}(\omega) = \frac{2M^{\mathrm{X}}}{3\pi k_{\mathrm{B}}T}\tanh\left(\frac{\hbar\omega}{2k_{\mathrm{B}}T}\right) \times \int_{-\infty}^{\infty}\mathrm{Re}[\langle v(0)v(t)\rangle^{\mathrm{X}}]\exp(-\mathrm{i}\omega t)\,\mathrm{d}t \tag{8}$$

where M^X is the mass of an atom X, k_B is the Boltzmann constant and T is the absolute temperature of water. It may be noted that $W^X(t)$ is expressed with $D^X(\omega)$:

$$W^X(t) = \frac{\hbar}{M^X}\int_0^\infty \frac{d\omega}{\omega} D^X(\omega)\left[\coth\left(\frac{\hbar\omega}{2k_BT}\right)\times(1-\cos\omega t) - i\sin\omega t\right]. \quad (9)$$

Consequently, once $D^X(\omega)$ for water is given, all the scattering functions can be determined immediately. This is the principal method of cross-section calculation in the present paper. In what follows, it is assumed that translational, rotational and intramolecular motions are independent. Namely, $I_s^X(Q,t)$, $W^X(t)$ and $D^X(\omega)$ may be written as

$$I_s^X(Q,t) = I_{sT}^X(Q,t)\times I_{sR}^X(Q,t)\times I_{sV}^X(Q,t) \quad (10)$$

$$W^X(t) = W_T^X(t) + W_R^X(t) + W_V^X(t) \quad (11)$$

$$D^X(\omega) = D_T^X(\omega) + D_R^X(\omega) + D_V^X(\omega) \quad (12)$$

where the subscripts T, R and V denote the translational, rotational and intramolecular-vibrational degrees of freedom, respectively.

2.2. Translational motion

The translational motion of a water molecule, for both H and O, may be represented by a jump diffusion process in a large time scale of $t \gg 1$ ps and an intermolecular vibration in an intermediate time scale of $t \sim 1$ ps. This may be written in the form

$$I_{sT}^X(Q,t) = I_{sd}^X(Q,t)\times I_{st}^X(Q,t) \quad (13)$$

where the subscripts d and t denote the jump diffusion and intermolecular vibration, respectively. For $W_T^X(t)$, it may be given by

$$W_T^X(t) = W_d^X(t) + \sum_{m=1}^{2}\varepsilon_{tm}^X W_{tm}^X(t) \quad (14)$$

where $m = 1, 2$ denote the bending and stretching modes, respectively, and ε_{tm}^X are the weight coefficients for each mode.

(a) The explicit expression for $W_d^X(t)$ is obtained from the following physical requirements: In a large time scale, a jump diffusion process with the self diffusion coefficient $D_t(T)$ and the residence time $\tau_0(T)$ becomes dominant [2,3]. On the other hand, in a very short time scale, a free-gas behavior for H or O will appear [9,10]. Hence we have

$$W_d^X(t) = 2\Gamma(Q)\left(\sqrt{t^2 - i\frac{\hbar t}{k_BT} + C(Q)^2} - C(Q)\right) \quad (15)$$

$$= \begin{cases} -i\dfrac{\hbar}{M_d^X(T)}t + \dfrac{k_BT}{M_d^X(T)}t^2 & (t \ll C(Q)) \\ 2\Gamma(Q)t & (t \gg C(Q)) \end{cases} \quad (16)$$

where

$$\Gamma(Q) = \frac{D_t(T)}{1 + Q^2 D_t(T)\tau_0(T)} \quad (17)$$

$$C(Q) = \frac{\Gamma(Q)M_d^X(T)}{k_BT}. \quad (18)$$

It is obvious that, for $t \gg C(Q)$ and small Q, $Q^2 W_d^X(t)/2 = Q^2 D_t(T)t$ showing a simple diffusion while, for $t \gg C(Q)$ and large Q, $Q^2 W_d^X(t)/2 = t/\tau_0(T)$ indicating the residence effect of molecules in a hydrogen-bonded network. This results in two different quasi-elastic scattering peaks: the former gives the half-width at half-maximum (HWHM) of $D_t(T)Q^2$ and the latter yields the saturated one of $1/\tau_0(T)$ with increasing Q. This is consistent with the recent experimental results by Teixeira et al. [2] and Cavatorta et al. [3]. It may be noted that $C(Q)$ is the delay time to distinguish between the jump diffusion process and the free gas behavior. The magnitudes of $C(Q)$ and also $\Gamma(Q)$ are determined through the model parameters $D_t(T)$, $\tau_0(T)$ and $M_d^X(T)$:

- The values of $D_t(T)$ as a function of T are assumed to obey the following Arrhenius behavior in the temperature range of interest:

$$D_t(T) = 258.2\times\exp\left(-2.108\frac{1000}{T}\right) \quad (\text{Å}^2\,\text{ps}^{-1}) \quad (19)$$

where the coefficients 258.2 and 2.108 are chosen by fitting Eq. (19) to the experimental results [30–35].

- According to the experiments [2,3], $\tau_0(T)$ shows non-Arrhenius behavior in the temperature range including super-cooled region below 0 °C. At temperatures above 0 °C, however, it exhibits nearly the Arrhenius behavior [23]:

$$\tau_0(T) = 1.548 \times 10^{-4} \times \exp\left(+2.648\,\frac{1000}{T}\right) \text{ (ps)}. \tag{20}$$

- The magnitude of an effective mass $M_{\mathrm{d}}^{\mathrm{X}}(T)$ is determined on the assumption of $C(Q) = \tau_0(T)$ at $Q = 0$. Then we have

$$M_{\mathrm{d}}^{\mathrm{X}}(T) = \frac{\tau_0(T) k_{\mathrm{B}} T}{D_{\mathrm{t}}(T)}. \tag{21}$$

(b) The intermolecular vibrations are simply expressed by the multi-phonon model [19],

$$W_{\mathrm{t}\,m}^{\mathrm{X}}(t) = 2\lambda_{\mathrm{t}\,m}^{\mathrm{X}}\left\{1 - \exp\left[-\frac{{\omega_{\mathrm{t}\,m}^{\mathrm{X}}}^2}{4} \times \left(t^2 - \mathrm{i}\,\frac{\hbar}{k_{\mathrm{B}} T}\,t\right)\right]\right\} \tag{22}$$

where the pre-factor $\lambda_{\mathrm{t}\,m}^{\mathrm{X}}$ is given by

$$\lambda_{\mathrm{t}\,m}^{\mathrm{X}} = \frac{2k_{\mathrm{B}} T}{M^{\mathrm{X}} {\omega_{\mathrm{t}\,m}^{\mathrm{X}}}^2} \tag{23}$$

and $\omega_{\mathrm{t}\,m}^{\mathrm{X}}$ $(m = 1, 2)$ are the characteristic frequencies of each vibrational mode. In a large time scale, $W_{\mathrm{t}\,m}^{\mathrm{X}}(t)$ tends to approach $\lambda_{\mathrm{t}\,m}^{\mathrm{X}}$ corresponding to the Debye–Waller factor in a crystal. The magnitudes of $\omega_{\mathrm{t}\,m}^{\mathrm{X}}$ are determined by use of the neutron experiments [24] and computer simulations [8] for $D_{\mathrm{T}}^{\mathrm{X}}(\omega)$.

(c) The whole expression for $D_{\mathrm{T}}^{\mathrm{X}}(\omega)$ is therefore obtained by the substitution of Eqs. (15) and (22) into Eq. (7) and the Fourier integration of the resultant VACF:

$$D_{\mathrm{T}}^{\mathrm{X}}(\omega) = D_{\mathrm{d}}^{\mathrm{X}}(\omega) + \sum_{m=1}^{2} \varepsilon_{\mathrm{t}\,m}^{\mathrm{X}} D_{\mathrm{t}\,m}^{\mathrm{X}}(\omega) \tag{24}$$

where

$$D_{\mathrm{d}}^{\mathrm{X}}(\omega) = \frac{4M^{\mathrm{X}}}{\pi\hbar\omega} \sinh\left(\frac{\hbar\omega}{2k_{\mathrm{B}} T}\right) D_{\mathrm{t}}(T)\alpha\omega K_1(\alpha\omega) \tag{25}$$

$$D_{\mathrm{t}\,m}^{\mathrm{X}}(\omega) = \frac{4\lambda_{\mathrm{t}\,m}^{\mathrm{X}} M^{\mathrm{X}}}{\sqrt{\pi}\hbar}\,\frac{\omega}{\omega_{\mathrm{t}\,m}^{\mathrm{X}}} \sinh\left(\frac{\hbar\omega}{2k_{\mathrm{B}} T}\right) \times \exp\left[-\left(\frac{\hbar\omega_{\mathrm{t}\,m}^{\mathrm{X}}}{4k_{\mathrm{B}} T}\right)^2\right] \times \exp\left[-\left(\frac{\omega}{\omega_{\mathrm{t}\,m}^{\mathrm{X}}}\right)^2\right] \tag{26}$$

with

$$\alpha = \sqrt{\left(\frac{\hbar}{2k_{\mathrm{B}} T}\right)^2 + C(0)^2} \tag{27}$$

and the modified Bessel function K_1 of second kind for order 1.

2.3. Rotational motion

Since a water molecule rotates in some degrees around the center of mass very near the position of O, the rotation of H is only treated while the one of O is simply expressed as $I_{\mathrm{s\,R}}^{\mathrm{O}}(Q,t) = 1$ and $W_{\mathrm{R}}^{\mathrm{O}}(t) = 0$. Then $I_{\mathrm{s\,R}}^{\mathrm{H}}(Q,t)$ is assumed to be composed of two different motions:

$$I_{\mathrm{s\,R}}^{\mathrm{H}}(Q,t) = I_{\mathrm{s\,RD}}^{\mathrm{H}}(Q,t) \times I_{\mathrm{s\,HR}}^{\mathrm{H}}(Q,t) \tag{28}$$

$$W_{\mathrm{R}}^{\mathrm{H}}(t) = W_{\mathrm{RD}}^{\mathrm{H}}(t) + \varepsilon_{\mathrm{HR}}^{\mathrm{H}} W_{\mathrm{HR}}^{\mathrm{H}}(t) \tag{29}$$

where the subscripts RD and HR denote the rotational diffusion and hindered rotation, respectively, and $\varepsilon_{\mathrm{HR}}^{\mathrm{H}}$ is the weight to be determined.

(a) In a large time scale, each molecule rotates in its respective direction, i.e. without any significant correlation to neighbouring molecules. This yields a quasi-elastic scattering whose HWHM is given by the rotational diffusion coefficient $D_{\mathrm{r}}(T)$ [13]. Accordingly,

the rotational diffusion may be represented by the Sear's expansion model [13]:

$$I^{\mathrm{H}}_{\mathrm{s\,RD}}(Q,t) = \frac{1}{A}\sum_{l=0}^{L}(2l+1)j_l^2(QR)F_l^{\mathrm{H}}(t) \quad (30)$$

where

$$A = \sum_{l=0}^{L}(2l+1)j_l^2(QR) \quad (31)$$

$L = 2$ is selected as the maximum order of expansion, R is the bond length between H–O atoms and $j_l(QR)$ is the spherical Bessel function for order l. The rotational correlation function $F_l^{\mathrm{H}}(t)$ is slightly modified to include a nearly free rotation at very short time:

$$F_l^{\mathrm{H}}(t) = \exp\left[-\frac{1}{2}\,Q^2 W^{\mathrm{H}}_{\mathrm{RD}\,l}(t)\right] \quad (32)$$

where

$$W^{\mathrm{H}}_{\mathrm{RD}\,l}(t) = 2\alpha_l(Q)\left(\sqrt{t^2 - \mathrm{i}\,\frac{\hbar t}{k_{\mathrm{B}}T} + c(Q)^2} - c(Q)\right) \quad (33)$$

$$\alpha_l(Q) = \frac{l(l+1)D_{\mathrm{r}}(T)}{Q^2} \quad (34)$$

$$c(Q) = \frac{\alpha_l(Q)M^{\mathrm{H}}_{\mathrm{r}}}{k_{\mathrm{B}}T}. \quad (35)$$

For $t \gg c(Q)$, $W^{\mathrm{H}}_{\mathrm{RD}\,l}(t)$ tends to approach $2\alpha_l(Q)t$ so that $F_l^{\mathrm{H}}(t) = \exp[-l(l+1)D_{\mathrm{r}}(T)t]$. The value of $D_{\mathrm{r}}(T)$ is given in terms of the rotational relaxation time $\tau_{\mathrm{RD}}(T)$ [2]:

$$D_{\mathrm{r}}(T) = \frac{1}{6\tau_{\mathrm{RD}}(T)} \quad (36)$$

where

$$\tau_{\mathrm{RD}}(T) = 0.0485 \times \exp\left(+\frac{80.7}{k_{\mathrm{B}}T}\right) \quad \text{(ps)}. \quad (37)$$

The expression (35) for the delay time $c(Q)$ is obtained by the requirement that $W^{\mathrm{H}}_{\mathrm{RD}\,l}(t)$ shows the free rotation behavior at very small t:

$$W^{\mathrm{H}}_{\mathrm{RD}\,l}(t) = -\mathrm{i}\,\frac{\hbar}{M^{\mathrm{H}}_{\mathrm{r}}}\,t + \frac{k_{\mathrm{B}}T}{M^{\mathrm{H}}_{\mathrm{r}}}\,t^2. \quad (38)$$

(b) In an intermediate time scale of, say, about 1 ps, the rotation is largely hindered so that only the hindered rotation with the characteristic frequency $\omega^{\mathrm{H}}_{\mathrm{HR}}$ is possible. This has been observed with the GFDs by experiment and simulations [24,8,11] with a significant peak around $\hbar\omega^{\mathrm{H}}_{\mathrm{HR}} = 80\,\mathrm{meV}$. Hence it may be approximately reproduced as

$$W^{\mathrm{H}}_{\mathrm{HR}}(t) = 2\lambda^{\mathrm{H}}_{\mathrm{HR}}\left\{1 - \exp\left[-\frac{{\omega^{\mathrm{H}}_{\mathrm{HR}}}^2}{4} \times\left(t^2 - \mathrm{i}\,\frac{\hbar}{k_{\mathrm{B}}T}\,t\right)\right]\right\} \quad (39)$$

where

$$\lambda^{\mathrm{H}}_{\mathrm{HR}} = \frac{2k_{\mathrm{B}}T}{M^{\mathrm{H}}{\omega^{\mathrm{H}}_{\mathrm{HR}}}^2}. \quad (40)$$

(c) The GFD $D^{\mathrm{X}}_{\mathrm{R}}(\omega)$ for the whole rotational motion is obtained by the procedure

$$W^{\mathrm{H}}_{\mathrm{R}}(t) = -\lim_{Q\to 0}\frac{2}{Q^2}\ln[I^{\mathrm{H}}_{\mathrm{s\,R}}(Q,t)] \quad (41)$$

and substituting the resultant $W^{\mathrm{H}}_{\mathrm{R}}(t)$ into Eqs. (7) and (8):

$$D^{\mathrm{H}}_{\mathrm{R}}(\omega) = D^{\mathrm{H}}_{\mathrm{RD}}(\omega) + D^{\mathrm{H}}_{\mathrm{HR}}(\omega) \quad (42)$$

with the following two components for $\omega \sim 0$ and $\omega^{\mathrm{H}}_{\mathrm{HR}}$:

$$D^{\mathrm{H}}_{\mathrm{RD}}(\omega) = 2\,\frac{M^{\mathrm{H}}}{M^{\mathrm{H}}_{\mathrm{r}}}\,\delta(\omega) \quad (43)$$

$$D^{\mathrm{H}}_{\mathrm{HR}}(\omega) = \frac{4\lambda^{\mathrm{H}}_{\mathrm{HR}}M^{\mathrm{H}}}{\sqrt{\pi}\hbar}\,\frac{\omega}{\omega^{\mathrm{H}}_{\mathrm{HR}}}\sinh\left(\frac{\hbar\omega}{2k_{\mathrm{B}}T}\right) \times\exp\left[-\left(\frac{\hbar\omega^{\mathrm{H}}_{\mathrm{HR}}}{4k_{\mathrm{B}}T}\right)^2\right] \times\exp\left[-\left(\frac{\omega}{\omega^{\mathrm{H}}_{\mathrm{HR}}}\right)^2\right]. \quad (44)$$

2.4. Intramolecular vibration

For the inner degree of freedom of a water molecule, the three vibrational normal modes, i.e. bending, stretching and asymmetric-stretching, are included. These modes are assumed to have narrow energy distributions centered in the normal-mode energies $\hbar\omega_{\mathrm{v}\,n}$ $(n=1,2,3)$ [4,5,8]:

$$D^{\mathrm{X}}_{\mathrm{v}\,n}(\omega)=\frac{1}{\sqrt{2\pi}\sigma_{\mathrm{v}\,n}}\exp\left[-\frac{\hbar^2(\omega-\omega_{\mathrm{v}\,n})^2}{2\sigma^2_{\mathrm{v}\,n}}\right] \tag{45}$$

where $\sigma_{\mathrm{v}\,n}$ is the standard deviation of vibrational energy for the mode n. Substituting Eq. (45) into Eq. (9) and using the conditions that $\sigma_{\mathrm{v}\,n}\ll\hbar\omega_{\mathrm{v}\,n}$ and $\hbar\omega_{\mathrm{v}\,n}\gg k_{\mathrm{B}}T$, we have

$$W^{\mathrm{X}}_{\mathrm{v}\,n}(t)=\frac{\hbar}{M^{\mathrm{X}}}\frac{1}{\omega_{\mathrm{v}\,n}}\left[1-\exp(\mathrm{i}\omega_{\mathrm{v}\,n}t)\times\exp\left(-\frac{\sigma^2_{\mathrm{v}\,n}}{2\hbar^2}\,t^2\right)\right]. \tag{46}$$

Hence, the WF $W^{\mathrm{X}}_{\mathrm{V}}(t)$ and the GFD $D^{\mathrm{X}}_{\mathrm{V}}(\omega)$ for intramolecular vibrations are written as

$$W^{\mathrm{X}}_{\mathrm{V}}(t)=\sum_{n=1}^{3}\varepsilon^{\mathrm{X}}_{\mathrm{v}\,n}W^{\mathrm{X}}_{\mathrm{v}\,n}(t) \tag{47}$$

$$D^{\mathrm{X}}_{\mathrm{V}}(\omega)=\sum_{n=1}^{3}\varepsilon^{\mathrm{X}}_{\mathrm{v}\,n}D^{\mathrm{X}}_{\mathrm{v}\,n}(\omega) \tag{48}$$

where $\varepsilon^{\mathrm{X}}_{\mathrm{v}\,n}$ are the weights to be determined.

2.5. Transition to free atom cross section

The present model is required to reproduce free atom cross section for epi-thermal neutrons ($E\gtrsim 1$ eV). This is equivalent to the requirement that $W^{\mathrm{X}}(t)$ describes the free gas motion of atom X at very short time ($t\sim 0.1$ fs):

$$W^{\mathrm{X}}(t)=W^{\mathrm{X}}_{\mathrm{d}}(t)+\sum_{m=1}^{2}\varepsilon^{\mathrm{X}}_{\mathrm{t}\,m}W^{\mathrm{X}}_{\mathrm{t}\,m}(t)+W^{\mathrm{H}}_{\mathrm{RD}}(t)+\varepsilon^{\mathrm{H}}_{\mathrm{HR}}W^{\mathrm{H}}_{\mathrm{HR}}(t)+\sum_{n=1}^{3}\varepsilon^{\mathrm{X}}_{\mathrm{v}\,n}W^{\mathrm{X}}_{\mathrm{v}\,n}(t) \tag{49}$$

$$\simeq -\mathrm{i}\,\frac{\hbar}{M^{\mathrm{X}}}\,t\quad\text{for}\quad t\sim 0. \tag{50}$$

Inserting the respective width functions into the right-hand side of Eq. (49) and expanding the result into the Taylor series around $t=0$, we obtain

$$\frac{M^{\mathrm{X}}}{M^{\mathrm{X}}_{\mathrm{d}}(T)}+\sum_{m=1}^{2}\varepsilon^{\mathrm{X}}_{\mathrm{t}\,m}+\frac{M^{\mathrm{H}}}{M^{\mathrm{H}}_{\mathrm{r}}}+\varepsilon^{\mathrm{H}}_{\mathrm{HR}}+\sum_{n=1}^{3}\varepsilon^{\mathrm{X}}_{\mathrm{v}\,n}=1. \tag{51}$$

It may be noted that the condition in Eq. (51) is also derived from the normalization of the total GFD to unity, namely

$$\int_0^\infty D^{\mathrm{X}}(\omega)\,\mathrm{d}\omega=1. \tag{52}$$

The model parameters appearing in Eq. (51) are determined by the following procedures:

(a) According to the GFD obtained by the molecular dynamics simulation [8], the total weights of intramolecular vibrations can be estimated to be 0.4 for H and 0.07 for O. Then we assume that

$$\varepsilon^{\mathrm{H}}_{\mathrm{v}\,1}=\varepsilon^{\mathrm{H}}_{\mathrm{v}\,2}=\varepsilon^{\mathrm{H}}_{\mathrm{v}\,3}=0.4/3 \tag{53}$$

$$\varepsilon^{\mathrm{O}}_{\mathrm{v}\,1}=\varepsilon^{\mathrm{O}}_{\mathrm{v}\,2}=\varepsilon^{\mathrm{O}}_{\mathrm{v}\,3}=0.07/3. \tag{54}$$

(b) The value of $M^{\mathrm{H}}/M^{\mathrm{H}}_{\mathrm{r}}$ is estimated to be ~ 0.0006 at most in order that $I^{\mathrm{H}}_{\mathrm{s}\,\mathrm{R}}(Q,t)$ is consistent with the one of molecular dynamics [10,11] in terms of its relaxation in the time range of 1–10 ps. This implies that the rotational diffusion is not significant, but cannot be neglected, at the water temperatures under consideration, as will be shown in Fig. 2(c).

(c) The remains, i.e. $\varepsilon^{\mathrm{X}}_{\mathrm{t}\,m}(T)$ $(\mathrm{X}=\mathrm{H},\mathrm{O};m=1,2)$ and $\varepsilon^{\mathrm{H}}_{\mathrm{HR}}(T)$, are determined as follows: First their magnitudes at 20 °C are found from the GFDs of molecular dynamics [8] and neutron experiment [24], so that $\varepsilon^{\mathrm{H}\,0}_{\mathrm{t}1}=0.016$, $\varepsilon^{\mathrm{H}\,0}_{\mathrm{t}2}=0.028$ and $\varepsilon^{\mathrm{H}\,0}_{\mathrm{HR}}=0.5548$. Then it is assumed that each fraction of $\varepsilon^{\mathrm{X}}_{\mathrm{t}\,m}(T)$ and $\varepsilon^{\mathrm{H}}_{\mathrm{HR}}(T)$ to the sum total of them is the same with the one at 20 °C. Finally, they may be written as a

function of T through $M_{\mathrm{d}}^{\mathrm{X}}(T)$:

$$\varepsilon_{\mathrm{t}\,m}^{\mathrm{H}}(T) = \frac{\varepsilon_{\mathrm{t}\,m}^{\mathrm{H}\,0}}{\varepsilon_{\mathrm{t}\,1}^{\mathrm{H}\,0} + \varepsilon_{\mathrm{t}\,2}^{\mathrm{H}\,0} + \varepsilon_{\mathrm{HR}}^{\mathrm{H}\,0}} \times \left(1 - \frac{M^{\mathrm{H}}}{M_{\mathrm{d}}^{\mathrm{H}}(T)} - \frac{M^{\mathrm{H}}}{M_{\mathrm{r}}^{\mathrm{H}}} - \sum_{n=1}^{3} \varepsilon_{\mathrm{v}\,n}^{\mathrm{H}}\right) \quad (m = 1, 2) \tag{55}$$

$$\varepsilon_{\mathrm{HR}}^{\mathrm{H}}(T) = \frac{\varepsilon_{\mathrm{HR}}^{\mathrm{H}\,0}}{\varepsilon_{\mathrm{t}\,1}^{\mathrm{H}\,0} + \varepsilon_{\mathrm{t}\,2}^{\mathrm{H}\,0} + \varepsilon_{\mathrm{HR}}^{\mathrm{H}\,0}} \times \left(1 - \frac{M^{\mathrm{H}}}{M_{\mathrm{d}}^{\mathrm{H}}(T)} - \frac{M^{\mathrm{H}}}{M_{\mathrm{r}}^{\mathrm{H}}} - \sum_{n=1}^{3} \varepsilon_{\mathrm{v}\,n}^{\mathrm{H}}\right) \tag{56}$$

$$\varepsilon_{\mathrm{t}\,m}^{\mathrm{O}}(T) = \frac{\varepsilon_{\mathrm{t}\,m}^{\mathrm{H}\,0}}{\varepsilon_{\mathrm{t}\,1}^{\mathrm{H}\,0} + \varepsilon_{\mathrm{t}\,2}^{\mathrm{H}\,0}} \left(1 - \frac{M^{\mathrm{O}}}{M_{\mathrm{d}}^{\mathrm{O}}(T)} - \sum_{n=1}^{3} \varepsilon_{\mathrm{v}\,n}^{\mathrm{O}}\right) \quad (m = 1, 2). \tag{57}$$

Note that the rotational motion for O is not taken into account.

(d) All the values of model parameters are listed up in Table 1.

3. Results and Discussion

3.1. Generalized frequency distribution

Fig. 1 shows the GFD $D(\omega)$ for a water at 20 °C as a function of $\hbar\omega$ up to 500 meV. It is defined by

$$D(\omega) = \frac{1}{1+\varepsilon} D^{\mathrm{H}}(\omega) + \frac{\varepsilon}{1+\varepsilon} D^{\mathrm{O}}(\omega) \tag{58}$$

where

$$\varepsilon = \frac{1}{2} \frac{\sigma_{\mathrm{coh}}^{\mathrm{O}} + \sigma_{\mathrm{inc}}^{\mathrm{O}}}{\sigma_{\mathrm{coh}}^{\mathrm{H}} + \sigma_{\mathrm{inc}}^{\mathrm{H}}} = 0.026. \tag{59}$$

The two components $D^{\mathrm{H}}(\omega)/(1+\varepsilon)$ and $\varepsilon D^{\mathrm{O}}(\omega)/(1+\varepsilon)$ are also shown in Fig. 1 by the dashed and dotted curves, respectively. By comparison with the results of neutron scattering [24] and molecular dynamics [8], the following characteristics are obvious: the translational diffusion near 0 meV, the translational bending and stretching vibrations at about 6 and 20 meV, the hindered rotation of a molecule around 70 meV, and the intramolecular vibrations at 200 and 463 meV. The hindered rotation is dominant only for $D^{\mathrm{H}}(\omega)/(1+\varepsilon)$ as can be also seen from the molecular dynamics results. On the other hand, the component $\varepsilon D^{\mathrm{O}}(\omega)/(1+\varepsilon)$ becomes significant for the translational motions at lower energies.

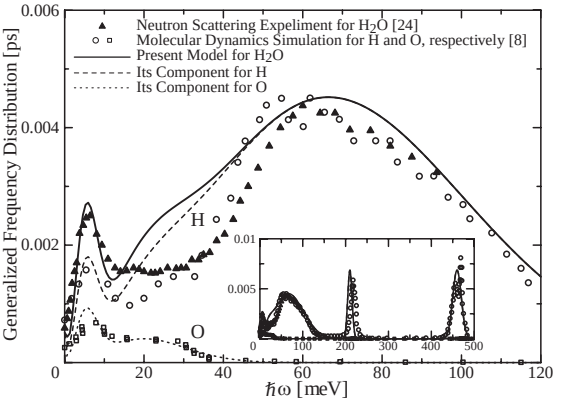

Fig. 1. The GFD of liquid water at 20 °C by the present model, the neutron scattering experiment [24] and the molecular dynamics simulations [8].

3.2. Intermediate scattering function

The ISFs $I_{\mathrm{s}}^{\mathrm{H}}(Q,t)$ at $Q = 1.16$ Å^{-1} for two different temperatures of 25 °C and 75 °C are calculated. The results are shown in Fig. 2(a) and compared with the experimental ones by Sakamoto et al. [25] although the experimentally-estimated mean squared displacements $\langle \Delta r^2 \rangle^{\mathrm{H}}$ are re-evaluated in terms of the ISF given by $\exp(-Q^2 \frac{1}{6} \langle \Delta r^2 \rangle^{\mathrm{H}})$. It can be seen from Fig. 2(a) that the present model shows relatively a gentle decay above ~ 0.5 ps. One possible reason is that $\langle \Delta r^2 \rangle^{\mathrm{H}}$ has been estimated on the assumption that the ISF is almost Gaussian in Q, namely, $I_{\mathrm{s}}^{\mathrm{H}}(Q,t) = \exp[-Q^2 D_{\mathrm{t}}(T) t]$. Hence there may be significant difference between the jump diffusion and the simple diffusion in this Q-t domain.

Fig. 2(b) shows the translational motion at 25 °C in terms of $I_{\mathrm{s\,T}}^{\mathrm{H}}(Q,t)$ for $Q = 1.16$ Å^{-1}. Also shown are the three relevant components: the jump diffusion by $I_{\mathrm{s\,d}}^{\mathrm{H}}(Q,t)$ and the intermolecular bending and stretching modes by $I_{\mathrm{s\,t}}^{\mathrm{H}}(Q,t)$. Various relaxations inherent in these processes are clearly

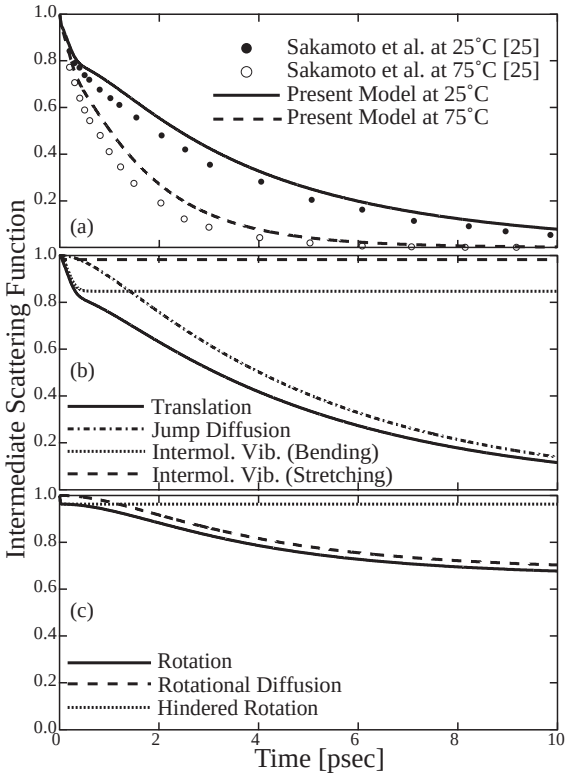

Fig. 2. The ISFs of H for $Q = 1.16$ Å^{-1}. (a) The calculated $I^{H}_{s}(Q,t)$ and the experimental values [25] at 25 °C and 75 °C. (b) $I^{H}_{sT}(Q,t)$ for translational dynamics. (c) $I^{H}_{sR}(Q,t)$ for rotational dynamics.

demonstrated in Fig. 2(b). It may be noted that slow dynamics by the jump diffusion arises in a time scale of ~ 10 ps and is largely dependent upon T through $D_t(T)$.

Fig. 2(c) indicates the ISF for rotational motion at 25 °C by $I^{H}_{sR}(Q,t)$ for $Q = 1.16$ Å^{-1}. It is further illustrated with the components for hindered rotation and rotational diffusion by $I^{H}_{sHR}(Q,t)$ and $I^{H}_{sRD}(Q,t)$, respectively. The former rapidly and slightly decays and approaches a constant value given by $\exp(-Q^2\lambda^{H}_{HR})$, while the latter gradually decreases till ~ 10 ps, owing to the slow relaxation as $\exp[-2D_r(T)t]$.

3.3. Double-differential cross section and self-scattering function

Fig. 3 shows the DDXs of water at 26 °C and $E = 304$ meV for four different scattering angles of $\theta = 30°$, $60°$, $75°$ and $90°$. In order to compare the calculated results with the experimental ones [26], the former are convoluted with the Gaussian resolution function $R(E')$ with the full-width at half-maximum (FWHM) of $\Delta E' = 30.4$ meV

$$R(E') = \frac{1}{\sqrt{2\pi}\sigma}\exp\left(-\frac{E'^2}{2\sigma^2}\right) \quad \text{with } \sigma = \Delta E'/2.35. \tag{60}$$

For $\theta = 30°$, the quasi-elastic neutron scattering (QENS) peak at $E' = 304$ meV is significant though accompanied with a slight asymmetry component by down scattering. This is due to the exchanges of small energies between incident neutrons and the slow dynamics of water molecules like the jump diffusion and the rotational diffusion. Also shown are the energy-loss inelastic

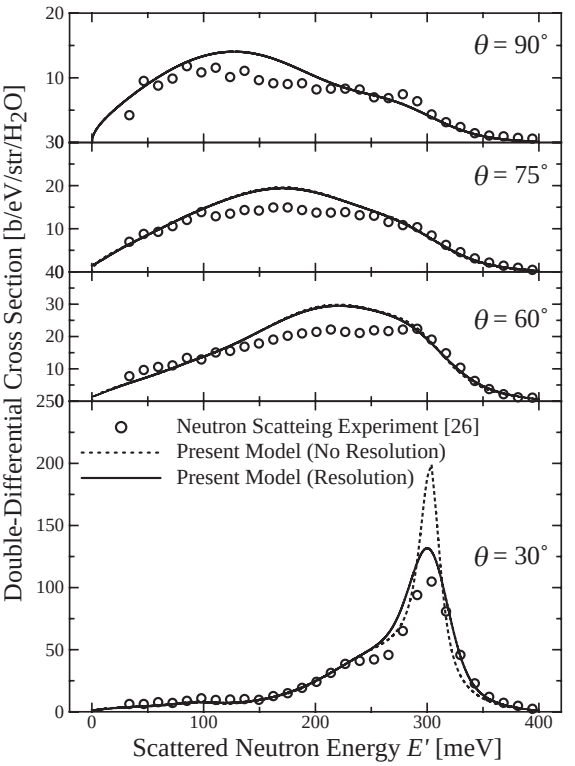

Fig. 3. The DDXs of water at 26 °C for $E = 304$ meV and $\theta = 30°$, $60°$, $75°$ and $90°$: the Harling's experimental results [26] and the present calculation with and without the energy resolution correction.

neutron scattering (INS) components: the shoulder at $E' \sim 220$ meV and the small peak at $E' \sim 100$ meV are caused by the excitations of hindered rotation and intramolecular bending mode, respectively. On the other hand, with an increase in θ, the INS tends to be dominant. It is mainly caused by the recoil scattering in free H and O atoms. Such an example is given of the DDX at $\theta = 90°$ with two broad peaks around $E' = 120$ and 270 meV.

Fig. 4 shows the DDXs of water at 20 °C for cold neutron scattering with $E = 1$ meV for four different scattering angles of $\theta = 15°$, 30°, 60° and 90°. The energy-gain INS is marked and broadens up to about 100 meV: the peak at 7 meV, the plateau around 25 meV and the tail from 60 to 100 meV arise from the de-excitations of the bending and stretching modes of intermolecular vibration and the hindered rotation, respectively. The QENS peaks are very sharp and high even at large θ, while the INS components are less sensitive to an increase of θ. This results in almost isotropic scattering in the energy range of cold neutrons, as will be shown in Fig. 7.

To characterize the QENS for various T and Q, a set of the scattering functions $S_s(Q,\omega)$ for Q ranging from 0.4 to 2 Å^{-1} is calculated. It is defined by

$$S_s(Q,\omega) = S_s^H(Q,\omega) + \varepsilon S_s^O(Q,\omega) \tag{61}$$

with the small contribution of $S_s^O(Q,\omega)$ by $\varepsilon = 0.026$. Typical results of $S_s(Q,\omega)$ at 20 °C and 75 °C are shown in Fig. 5. The QENS peaks are almost Lorentzian as described by the present jump diffusion model. With increasing Q and T, the QENS peaks broaden and become low. To evaluate such Q-T dependence of the peaks, their HWHMs are calculated and shown in Fig. 6 as a function of Q^2 at 5, 12, 20, 45, 56 and 75 °C. Also shown are the experimental results [2,3,23] and the calculated ones with only the jump diffusion process. The present model by the solid curves are in satisfactory agreement with the experiments for all temperatures shown. The jump diffusion results by the dashed curves, however, are always smaller than the others especially for $Q^2 > 2$ Å^{-2}, though they tend to saturate to $\hbar/\tau_0(T)$ for larger Q. This indicates that the HWHM under discussion is composed of both QENS and INS components. In fact, the experimental results of Teixeira et al. [2] and Cavatorta et al. [3] have been obtained by estimating the translational jump diffusion contribution from the QENS components, thus yielding similar behavior to the calculated jump diffusion ones. On the other hand, those of Blanckenhagen [23] have been derived by fitting a Lorentzian–Gaussian-convolution function to the experimental QENS peaks, so that the INS component is adequately included even at high T and Q.

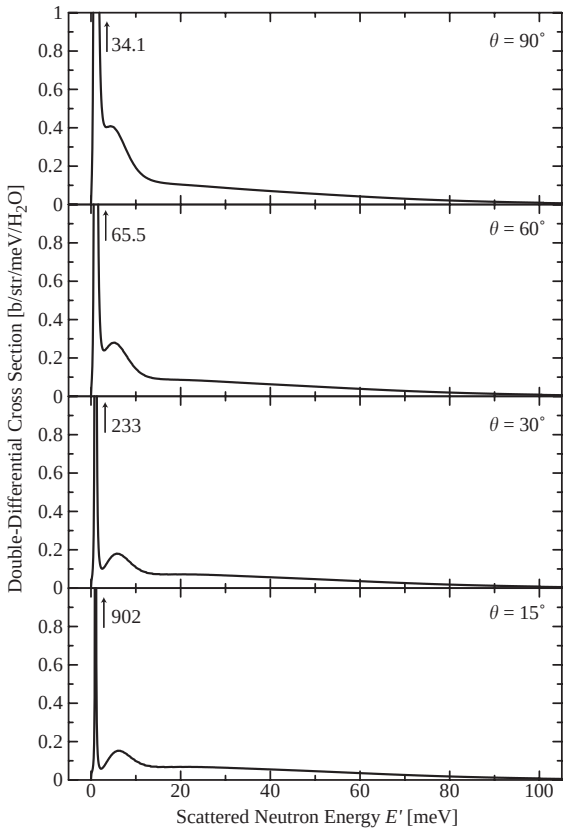

Fig. 4. The DDXs of water at 20 °C for $E = 1$ meV and $\theta = 15°$, 30°, 60° and 90°.

3.4. Angular distribution

The AD of neutron scattering has been calculated numerically by

$$\frac{d\sigma(E,\theta)}{d\Omega} = \int_0^\infty \frac{d^2\sigma(E',E,\theta)}{d\Omega\, dE'}\, dE'. \tag{62}$$

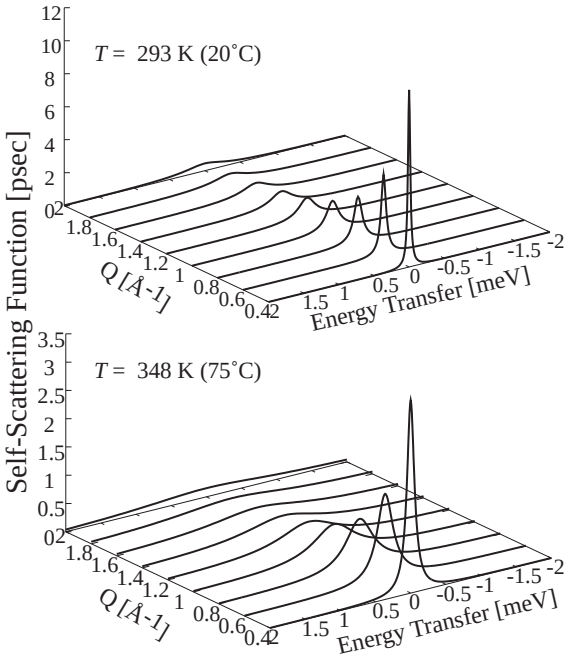

Fig. 5. A set of $S_s(Q,\omega)$ for water at 20 °C (the top figure) and 75 °C (the bottom one) for $E = 3.2$ meV and Q ranging from 0.4 to 2.0 Å^{-1}.

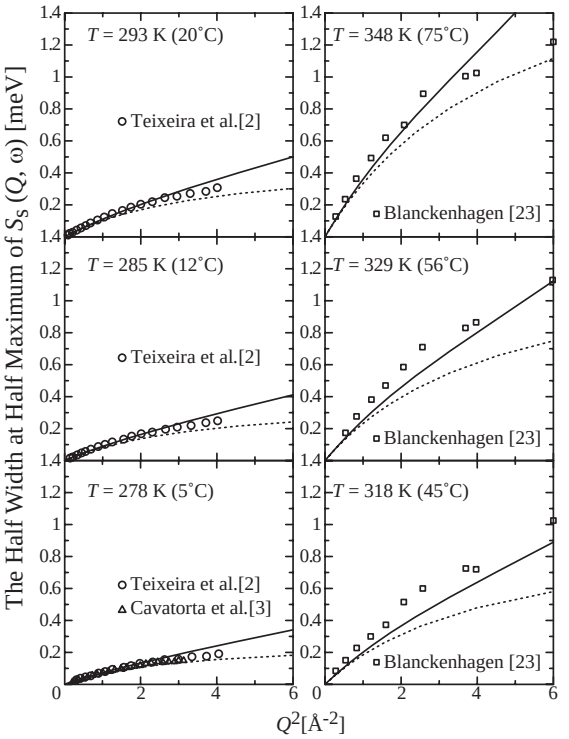

Fig. 6. The HWHMs of the QENS peak of $S_s(Q,\omega)$ at 5 °C, 12 °C, 20 °C, 45 °C, 56 °C and 75 °C: the experimentally-estimated results [2,3,23] by ○, △ and □, the present model by solid curves and the jump diffusion model by dotted curves.

Fig. 7 shows the results for $E = 10$ eV (epi-thermal), 20 meV (thermal) and 1 meV (cold), together with the experimental ones of thermal neutron [27,28]. For an epi-thermal neutron, the almost forward scattering is found by the recoil scattering in free H atom: The result of $\sigma_s^H \cos\theta$ for $\theta < 90°$ is also plotted by the dashed curve. The small backward component above 90° may be due to a nearly isotropic scattering in free O atom. On the contrary, the cold neutron scattering shows an nearly isotropic behavior though a backward scattering slightly appears by the de-excitations of intermolecular vibrations and hindered rotation. The result of thermal neutron indicates a mid-behavior between the above extremes and is consistent with the experimental ones [27,28] in the whole range of θ shown.

3.5. Total cross section

The TSX $\sigma_s(E)$ for water is calculated by numerically integrating the DDX with respect to θ and E':

$$\sigma_s(E) = 2\pi \int_{-1}^{1} d(\cos\theta) \int_0^{\infty} dE' \frac{d^2\sigma(E', E, \theta)}{d\Omega\, dE'}. \quad (63)$$

Also the total absorption cross section $\sigma_a^H(E)$ for two H atoms is found by a $1/v_n$ law with a neutron's velocity v_n:

$$\sigma_a^H(E) = 2 \times 0.3326 \times \sqrt{\frac{25.0}{E}} \quad \text{(b)} \quad (64)$$

with E in meV. Hence the total cross section $\sigma_t(E)$ of H_2O is expressed by $\sigma_t(E) = \sigma_s(E) + \sigma_a^H(E)$. The results of $\sigma_t(E)$ and $\sigma_a(E)$ at 20 °C and 75 °C are shown in Fig. 8 in the energy range from 0.1 μeV to 10 eV. Also shown are the experimental $\sigma_t(E)$ from the BNL-325 [29] and the calculated one by the Nelkin model [15] at room temperature. The present model is in good agreement with the experiment over the whole range of E. At lower E

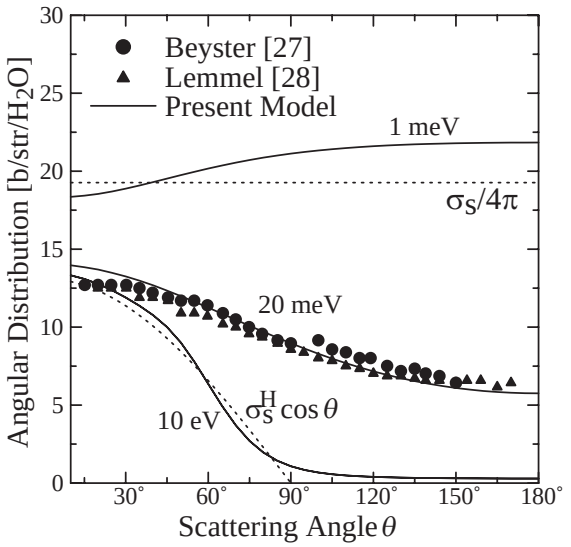

Fig. 7. The calculated ADs of water at 20 °C for $E = 1, 20$ meV and 10 eV, together with the experimental results [27,28] for $E = 20.4$ meV. The forward scattering in H and the isotropic scattering in H_2O are also shown by dashed curves: $\sigma_s^H = 20.4$ b and $\sigma_s = 242$ b.

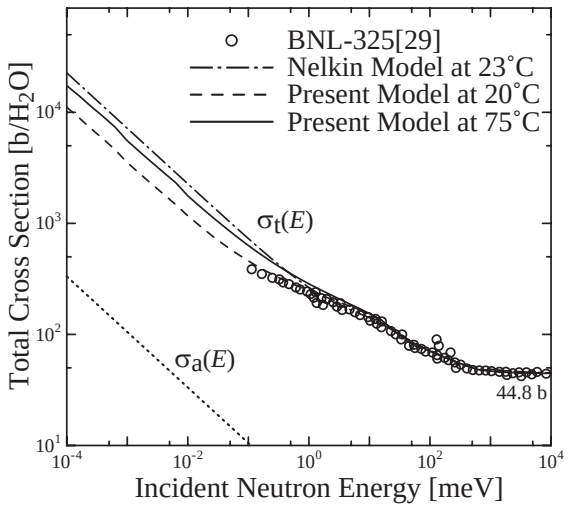

Fig. 8. The total cross sections $\sigma_t(E)$ of a water molecule by the present model at 20 °C and 75 °C and the Nelkin model [15] at 23 °C. Also shown are the experimental $\sigma_t(E)$ from the BNL-325 [29] by open circles and $\sigma_a(E)$ by dotted curve.

(< 10 meV), the slow dynamics of water has an influence on $\sigma_t(E)$ by the slight departure from a $1/v_n$ behavior, which cannot be seen from the Nelkin model. With increasing T, there appears much more up-scattering due to the de-excitations of various vibrational motions. In the energy range above 1 eV, $\sigma_t(E)$ approaches the free atom cross-section of 44.8 b for H_2O.

4. Concluding remarks

A cross-section model of liquid water has been successfully developed to be able to cover the wide ranges of incident neutron energy from 0.1 μeV (ultracold) to 10 eV (epi-thermal) and water temperature from 0 °C to 100 °C. This is accomplished by a full description of microscopic dynamics of water concerning the translational, rotational and intramolecular degrees of freedom: namely, jump diffusion and rotational relaxation in a large time scale ($t \gtrsim 1$ ps), intermolecular vibrations with bending and stretching modes, hindered rotation in an intermediate time scale (0.1 fs $\lesssim t \lesssim 1$ ps), and free gas behavior in a very short time scale ($t \lesssim 0.1$ fs). Accordingly, the dynamics of molecules inherent in liquid water has been fully discussed by quantitative comparison with both neutron-scattering and molecular-dynamics results [2,3,8,23–29]. As a result of the present study, the followings may be expected:

- The present cross-section model allows us to generate advanced neutron cross-section libraries of water (H_2O) at various temperatures. Such libraries would be valuable for many practical purposes in the fields of neutron science and nuclear engineering.
- The present dynamics model may be generalized to study heavy water (D_2O) dynamics in terms of coherent and incoherent inelastic scattering.
- The model may serve as a useful aid in understanding various results by neutron scattering study and computer simulation for liquid water.

Acknowledgements

The authors are grateful to Dr. S. Tasaki who has made very valuable suggestions for developing the present cross-section model.

References

[1] S.H. Chen, J. Teixeira, R. Nicklow, Phys. Rev. A 26 (6) (1982) 3477.
[2] J. Teixeira, M.-C. Bellissent-Funel, S.H. Chen, A.J. Dianoux, Phys. Rev. A 31 (3) (1985) 1913.
[3] F. Cavatorta, A. Deriu, D.D. Cola, H.D. Middendorf, J. Phys.: Condens. Matter 6 (23A) (1994) A113.
[4] M.-C. Bellissent-Funel, J. Teixeira, J. Mol. Structure 250 (1991) 213.
[5] S.-H. Chen, K. Toukan, C.-K. Loong, D.L. Price, Phys. Rev. Lett. 53 (14) (1984) 1360.
[6] K. Toukan, M.A. Ricci, S.-H. Chen, C.-K. Loong, D.L. Price, J. Teixeira, Phys. Rev. A 37 (7) (1988) 2580.
[7] R.W. Impey, P.A. Madden, I.R. McDonald, Mol. Phys. 46 (3) (1982) 513.
[8] G.C. Lie, E. Clementi, Phys. Rev. A 33 (4) (1986) 2679.
[9] J.J. Ullo, Phys. Rev. A 36 (2) (1987) 816.
[10] D.D. Cola, A. Deriu, M. Sampoli, A. Torcini, J. Chem. Phys. 104 (11) (1996) 4223.
[11] L. Liu, A. Faraone, S.-H. Chen, Phys. Rev. E 65 (2002) 041506.
[12] K.S. Singwi, A. Sjölander, Phys. Rev. 119 (3) (1960) 863.
[13] V.F. Sears, Canad. J. Phys. 44 (1966) 1299.
[14] M. Bee, Quasielastic Neutron Scattering: Principles and Applications in Solid State Chemistry, Biology and Material Science, Adam Hilger, Bristol, 1988.
[15] M. Nelkin, Phys. Rev. 119 (2) (1960) 741.
[16] H.L. McMurry, G.J. Russel, R.M. Brugger, Nucl. Sci. Eng. 25 (1966) 248.
[17] J.U. Koppel, Reactor Physics in the Resonance and Thermal Regions, MIT Press, Cambridge, MA, 1967.
[18] Y. Gotoh, H. Takahashi, Nucl. Sci. Eng. 45 (1971) 126.
[19] N. Morishima, Y. Aoki, Ann. Nucl. Energy 22 (3/4) (1995) 147.
[20] J.R. Granada, Phys. Rev. B 31 (7) (1985) 4167.
[21] J.R. Granada, Phys. Rev. B 32 (11) (1985) 7555.
[22] J.R. Granada, V.H. Gillette, R.E. Mayer, Phys. Rev. A 36 (12) (1987) 5594.
[23] P.V. Blanckenhagen, Berichte der Bunsengesellschaft für Physikalische Chemie 76 (9) (1972) 891.
[24] M.-C. Bellissent-Funel, S.H. Chen, J.-M. Zanotti, Phys. Rev. E 51 (5) (1995) 4558.
[25] M. Sakamoto, B.N. Brockhouse, R.G. Johnson, N.K. Pope, J. Phys. Soc. Japan 17 (Suppl. B-II) (1962) 370.
[26] O.K. Harling, J. Chem. Phys. 50 (12) (1969) 5279.
[27] J.R. Beyster, Nucl. Sci. Eng. 31 (1968) 254.
[28] V.H.-D. Lemmel, Nukleonik 7 (1965) 265.
[29] D.I. Garber, R.R. Kinsey, Neutron Cross Sections BNL-325 Volume II, 3rd Edition, Curves, National Neutron Cross Section Center, Brookhaven National Laboratory, January 1976.
[30] J.H. Simpson, H.Y. Carr, Phys. Rev. 111 (5) (1958) 1201.
[31] K.T. Gillen, D.C. Douglass, M.J.R. Hock, J. Chem. Phys. 57 (1972) 5117.
[32] R. Mills, J. Phys. Chem. 77 (5) (1973) 685.
[33] L.A. Woolf, J. Chem. Soc. Faraday I 71 (1975) 784.
[34] L.A. Woolf, J. Chem. Soc. Faraday I 72 (1976) 1267.
[35] K.R. Harris, L.A. Woolf, J. Chem. Soc. Faraday I 76 (1980) 377.